DOI: https://doi.org/10.57233/ijsgs.v10i3.699

ISSNp: 2488-9229; **ISSNe:** 3027-1118

IJSGS FUGUSAU VOL. 10 (3) **WEBSITE: https://fugus-ijsgs.com.ng**

INTERNATIONAL JOURNAL OF SCIENCE FOR GLOBAL SUSTAINABILITY

(A PUBLICATION OF FACULTY OF SCIENCE, FEDERAL UNIVERSITY GUSAU, NIGERIA)

Structural and Electrical Properties of Fluorine doped Tin oxide (FTO) Thin Film Deposited by Spin Coating Technique

[1]Abdullahi, S., [1]Sani, F., Buda, S., [2]Idris, A. T., *[3]Aliyu, M. W., and [1]Abdullahi, B.

[1]Department of Physics, Usmanu Danfodiyo University, Sokoto, Nigeria

[2]Department of Computer Science, Usmanu Danfodiyo University, Sokoto, Nigeria

[3]Department of Science Technology, Waziri Umaru Federal Polytechnic, Kebbi State, Nigeria,

***Corresponding Author's E-mail & Phone No:** muhammadamirat@gmail.com; +2347037981592

Received on: August, 2024 **Revised and Accepted on:** September, 2024 **Published on:** October, 2024

ABSTRACT

Fluorine-Doped Tin Oxide (FTO) thin films were deposited on a glass substrate using the spin coating technique and then annealed in both open air and nitrogen environments at temperatures between 500ºC and 600°C. This study examined how annealing temperature affects the structural and electrical properties of the films. X-ray diffraction (XRD) analysis showed that the films had a polycrystalline structure, predominantly with the (110) plane. As the annealing temperature is increased, the crystal size also increased, leading to lower dislocation density and higher electron mobility. The resistivity of the films decreased with higher annealing temperatures, reaching its lowest value at 600°C. These findings indicate that annealing temperature is crucial for optimizing the structural and electrical properties of FTO thin films made via spin coating. The optimal annealing conditions were found to be 600°C in open air, resulting in a resistivity of 2.47×10^{-3} Ω-cm, sheet resistance of 1.08×10^{-2} Ω/square, the largest grain size of 18.41 nm, and the lowest values for dislocation density (2.95×10^{15} lines/cm^2) and micro-strain (1.97×10^{-3}).

Keywords: FTO thin film, Spin Coating, Annealing Temperature, Grain size, Dislocation Density

1.0 INTRODUCTION

Transparent conducting oxides (TCOs) are the most essential type of electrically conductive materials, known for their low light absorption (Adedokun, 2019). TCOs possess unique properties defined by their deposition method, preparation conditions, and the availability of semiconductors with a band gap of approximately ≥ 3.1 eV (Sabzehmeidani *et al*., 2024). These materials combine high electrical conductivity with visible transparency, making them valuable for opto-electric devices such as electrochromic cells and solar cells (El-Jouad *et al*., 2023). Examples of TCOs include indium tin oxide (ITO), cadmium oxide (CdO), tin oxide (SnO_2), indium oxide (IO), undoped zinc oxide (ZO), and fluorine-doped tin oxide (FTO) (Gholami *et al*., 2023).

Fluorine doped tin oxide (FTO) is an n-type semiconductor with a range of applications, including transparent conducting electrodes, liquid crystal displays, photovoltaic cells, thin-film heaters, and solid-state gas sensors. Various technologies have been successfully employed to create high-quality films for these devices, such as chemical vapor deposition (CVD) (Elanjeitsenni *et al*., 2023), spray pyrolysis (Gholami *et al*., 2023), sol-gel dip coating (Park *et al*., 2024), and sol-gel spin coating (Ethiraj *et al*., 2021). FTO thin films have been produced using a variety of deposition methods, including CVD (Elanjeitsenni *et al*., 2023), sol-gel processing (Tofighi *et al*., 2019), sputtering (Harilal *et al*., 2022), and pulsed laser deposition (PLD) (Dharmaprakash, 2023). Among these methods, spin coating was used in this study due to its advantages such as low cost, and control over morphology and stoichiometry (Kahatta, 2016).

In this study, FTO thin films were deposited using the sol-gel spin coating technique while varying the annealing temperature. This method is straightforward, efficient, and cost-effective, requires minimal space, and does not necessitate a high vacuum. Additionally, it can produce films with uniform and controllable thickness as well as desirable microstructures (Padvi,2021). Structural properties were confirmed using an X-ray diffractometer, while electrical properties were measured using four-point probe measurements.

2.0 MATERIALS AND METHODS

2.1 Substrate Cleaning and Sample Preparation

Commercial microscopic glass slides (1.45 × 75 × 25 mm^3) were used as substrates for the spin coating deposition of FTO thin films. Before deposition, the substrates underwent a thorough cleaning process: they were heated in chromic acid for 2 hours, rinsed with single distilled water (SD) and deionized water (DI), degreased with acetone, ultrasonically cleaned with DI water, and then air-dried.

2.2 Precursor Preparation

DOI: https://doi.org/10.57233/ijsgs.v10i3.699

ISSNp: 2488-9229; **ISSNe:** 3027-1118

IJSGS FUGUSAU VOL. 10 (3) **WEBSITE: https://fugus-ijsgs.com.ng**

The tin precursor solution was prepared by dissolving 12.0 g of tin chloride pentahydrate ($SnCl_4 \cdot 5H_2O$, from Sigma Aldrich) in 100 ml of ethanol and stirring at 3000 rpm for 30 minutes. To create the fluorine doping solution, 2.0 g of NH_4F were dissolved in 4.0 ml of distilled water and vigorously stirred for 30 minutes to form a homogeneous mixture. This doping solution was then mixed with the tin precursor solution using a dropper, and the mixture was stirred for an additional 30 minutes. The ratio of $SnCl_4 \cdot 5H_2O$ to NH_4F was set at 2 weight percent.

2.3 Thin Film Deposition

The thin films were prepared using the spin coating technique with a spin coater (Model: HO-TH-05). The cleaned glass substrate was positioned on the spin coater's vacuum chuck, ensuring it was securely held in place to prevent any movement during spinning. A few drops of the FTO solution were applied to the center of the substrate using a micropipette. The deposition parameters were set with a spin speed of 2000 to 3000 rpm and spin duration of 30 to 90 seconds. After coating, the substrates were placed on a hot plate at 200°C for 10 minutes.

2.4 Annealing the Samples

Before characterizing the samples to determine their properties, they were heated at temperatures of 500°C, 550°C, and 600°C, except for the as-deposited sample. Samples marked F_1, F_2, and F_3, each with a uniform average thickness of 147 nm, were heat-treated in a furnace in open air for 30 minutes and then allowed to slowly cool to room temperature. Samples marked F_4, F_5, and F_6, also with a uniform average thickness of 147 nm, were annealed in a nitrogen atmosphere for 30 minutes. Sample F_7 was kept as the as-deposited sample.

2.5 Characterization of Thin Films

The annealing process was conducted at temperatures of 500°C, 550°C, and 600°C for 30 minutes in a furnace in both open air and nitrogen environments. The structural properties of the FTO thin films were characterized using X-ray diffraction (XRD) (DD-15.5 standard diffractometer) equipped with a Cu source (wavelength λ = 1.5418 Å) over the range of 2θ = 20–80°, with a scan speed of 0.8 degrees per minute and a scan step of 0.02. Surface morphology was examined while the thickness of the FTO thin layer was measured with a profilometer (Dektak XTL Stylus). The electrical properties of the samples were analyzed using a four-point probe (FPP5000).

2.6 Method of Calculation

Bragg's Law is used for the calculations and is given by the equation:

$$2d\sin\theta = n\lambda \quad (1)$$

Where, θ is the glancing angle, λ is the wavelength, and d is the spacing between consecutive parallel planes. The average crystallite sizes of the deposited FTO thin films can be calculated using Scherrer's equation (Equation 2) (Kadhim et al., 2022).

$$D = \frac{0.9\lambda}{\beta \cos\theta} \quad (2)$$

Here, D represents the crystal size, λ is the wavelength of the x-ray, and β is the full width at half maximum (FWHM) measured in radians.

The lattice parameters for the tetragonal phase can be calculated using the relation in Equation (3) (Kim, 2020).

$$\frac{1}{d^2} = \frac{h^2+k^2}{a^2} + \frac{1}{c^2} \quad (3)$$

In this equation, d represents the interplanar distance, and (*h, k, l*) are the Miller indices for the Bragg reflection.

The micro-strain (ε) and dislocation density (δ) of the deposited FTO thin films can be calculated using Equations 4 and 5, respectively (Ibrahim *et al.*, 2022).

$$\varepsilon = \frac{\beta \cos\theta}{4 \sin\theta} \quad (4)$$

$$\delta = \frac{1}{D^2} \quad (5)$$

The sheet resistance can be computed using equation 6 (Shekhirev *et al*, 2021):

$$R_S = \frac{\pi}{Ln2}\left(\frac{V}{I}\right) = 4.53\frac{V}{I} \quad (6)$$

Resistivity can also be expressed as in equation (7) (Muhammad and Alwan, 2020).

$$\rho = R_S \times t \quad (7)$$

3.0 RESULTS AND DISCUSSION

3.1 Structural Properties FTO thin films

Recent advancements in XRD profile analysis have enabled the revelation of micro-structural details such as micro-strain, crystallite size, and dislocation density. Figure 1 displays the XRD patterns of fluorine-doped tin oxide thin films annealed at different temperatures (as-deposited, 500°C, 550°C, and 600°C) in open air for one hour. The angle of incidence varied from 10° to 80°. The XRD results indicate that the as-deposited film is amorphous, showing no diffraction peaks. According to Ahmad *et al.* (2021), this amorphous structure occurs because the constituent atoms and molecules accumulate at random sites in the lattice due to insufficient heat energy to activate vibrational motion to settle at sites of minimum energy.

DOI: https://doi.org/10.57233/ijsgs.v10i3.699

ISSNp: 2488-9229; **ISSNe:** 3027-1118

IJSGS FUGUSAU VOL. 10 (3) **WEBSITE: https://fugus-ijsgs.com.ng**

The XRD patterns of FTO thin films annealed at 500°C, 550°C, and 600°C exhibit similar peaks with varying intensities. For the sample annealed at 600°C, four major peaks appeared at 2θ = 26.54°, 37.86°, 51.46°, 61.72°, and 65.8°, corresponding to the (110), (111), (200), (211), and (301) crystallographic planes, respectively. For the sample annealed at 550°C, peaks were observed at 2θ = 26.54°, 37.99°, 51.73°, 61.72°, and 65.18°, and for the sample annealed at 500°C, peaks appeared at 2θ = 26.66°, 37.34°, 51.73°, 61.12°, and 65.12°. These results align with studies by Abdel Galil *et al* (2021); Ethiraj *et al* (2021); and Kajal *et al.* (2023). As the annealing temperature increases, the XRD patterns indicate a polycrystalline tetragonal structure.

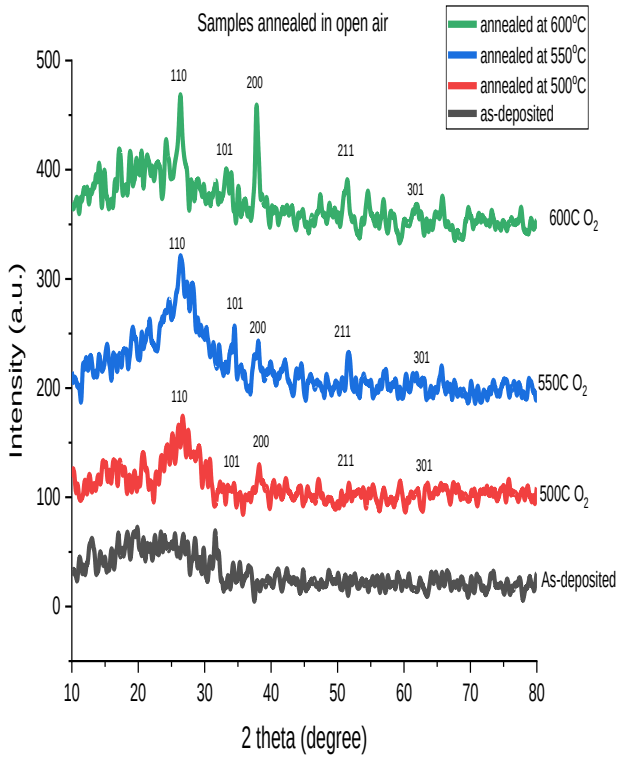

Figure 1: XRD Patterns of FTO Thin Films at various Annealing Temperatures in Open Air

Figure 2 shows the XRD patterns of nitrogen-annealed FTO films at various annealing temperatures. From the figure, the peaks correspond to the (110), (101), (200), (211), and (301) crystallographic planes, located at 26.42°, 33.70°, 37.99°, 51.82°, and 65.88°, respectively. These diffraction lines match the tetragonal rutile phase of SnO_2, as per ICCD card No. 41-1445. The XRD patterns for the deposited thin films (Figures 1 and 2) show no peaks consistent with other phases of tin oxide or tin fluorine oxides. This can be attributed to the close ionic radii of F^- (1.34 Å) and O^{2-} (1.35 Å), allowing F^- ions to substitute O^{2-} ions in the SnO_2 matrix without altering the tetragonal crystal structure (Badawi *et al.*, 2022). The XRD pattern of the as-deposited thin film shows no clear peaks, indicating an almost amorphous structure. As the annealing temperature increases, the XRD patterns indicate a polycrystalline phase, consistent with the findings of Adedokun *et al.* (2019).

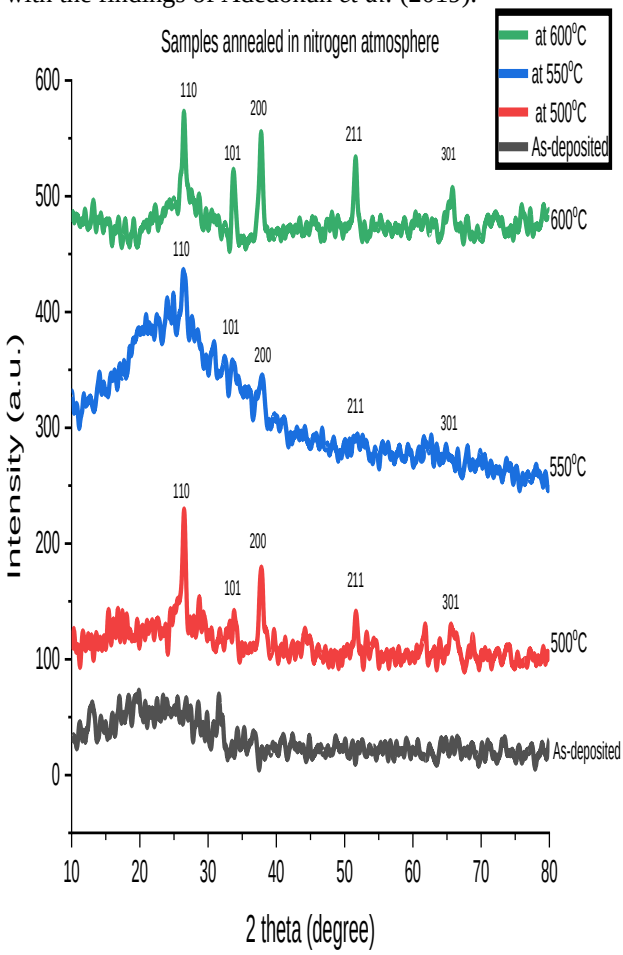

Figure 2: XRD Patterns of FTO Thin Films at various Annealing Temperatures in Nitrogen Atmosphere.

Based on the XRD spectra, the interplanar spacing, lattice constant, crystal size, lattice strain, and dislocation density of FTO films annealed in different environments and at various annealing temperatures were calculated for the (110) prominent reflection plane. The results are presented in Table 1.

The lattice constants are consistent with the bulk values (a = 4.73 Å and c = 3.18 Å). The grain sizes in the films increase with higher annealing temperatures in both environments. This increase is primarily due to the enhanced thermal energy promoting crystallization, recrystallization, and grain growth (Yu *et al.*, 2019).

DOI: https://doi.org/10.57233/ijsgs.v10i3.699

ISSNp: 2488-9229; **ISSNe:** 3027-1118

IJSGS FUGUSAU VOL. 10 (3) **WEBSITE: https://fugus-ijsgs.com.ng**

Structural parameters, such as dislocation density (δ) and micro-strain (ε), decrease with rising annealing temperatures, likely due to a reduction in lattice imperfections.

The Full Width at Half Maximum (FWHM) values of FTO thin films increase when comparing nitrogen to open air environments, suggesting that the crystal quality of the films improves with the annealing atmosphere. The FWHM and intensity of the XRD patterns are related to the crystallinity of the samples. Films with higher crystallinity exhibit more pronounced diffraction peaks and lower FWHM values, although this can also be affected by the film thickness (Khemiri *et al.*, 2020).

From the values in Table 1, it can be seen that the Full Width at Half Maximum (FWHM) of the diffraction peak from the (110) plane narrows as the annealing temperature increases in both atmospheres. This indicates an improvement in grain growth, as the crystallite sizes of the FTO thin films also increase with higher annealing temperatures.

Table 1 shows, that the dislocation density (δ) of FTO films annealed in open air decreases with increasing annealing temperature, with values ranging from 4.03 to 2.95 × 10^{15} lines/cm². This reduction in dislocation density indicates that higher annealing temperatures help decrease the number of defects. Annealing reduces crystal defects, such as dislocations and strain, thereby enhancing the crystallinity of the FTO films (Rahman *et al.*, 2021). Additionally, Table 1 reveals that the highest dislocation density, δ = 6.37 × 10^{15} lines/cm², is observed in films annealed in a nitrogen atmosphere, while the lowest dislocation density is δ = 4.06 × 10^{15} lines/cm².

Table 1 shows, that micro-strain (ε) decreases as the annealing temperature increases, with values in the range of ~10^{-3}. This suggests that higher annealing temperatures improve the crystallinity of the FTO films (Rahman *et al.*, 2021). Specifically, the highest micro-strain is 2.30 × 10^{-3} and the lowest is 1.97 × 10^{-3} per unit area for samples annealed in open air. For samples annealed in a nitrogen atmosphere, the highest micro-strain is 2.89 × 10^{-3} and the lowest is 2.31 × 10^{-3} per unit area.

Table 1: Structural Parameters of FTO Thin Films Annealed at various Temperatures.

Samples	**2θ (°)**	**d (Å)**	**a (Å)**	**c (Å)**	**FWHM (°)**	**D (nm)**	**δ x10^{15} (lines cm^{-2})**	**ε x10^{-3}**
As deposited	26.80	3.3239	4.7489	3.1800	1.0739	7.95	15.85	4.56
FTO 500℃ in air	26.00	3.3142	4.7489	3.1800	0.5502	15.75	4.03	2.30
FTO 550℃ in air	26.42	3.3708	4.7489	3.1800	0.5262	16.67	3.60	2.17
FTO 600℃ in air	26.42	3.3708	4.7489	3.1800	0.5011	18.41	2.95	1.97
FTO 500℃ in N_2	26.36	3.3783	4.7489	3.1800	0.7579	13.04	5.88	2.78
FTO 550℃ in N_2	26.36	3.3783	4.7489	3.1800	0.7433	12.53	6.37	2.89
FTO 600℃ in N_2	26.46	3.3658	4.7489	3.1800	0.6161	15.70	4.06	2.31

DOI: https://doi.org/10.57233/ijsgs.v10i3.699

ISSNp: 2488-9229; **ISSNe:** 3027-1118

IJSGS FUGUSAU VOL. 10 (3) **WEBSITE: https://fugus-ijsgs.com.ng**

3.2 Electrical Properties of FTO Thin Films

The resistivity of the films was measured using the four-point probe method. Figure 4 depicts the variation of resistivity (ρ) of FTO thin films with annealing temperature for two different annealing atmospheres: open air and nitrogen.

The figure illustrates the resistivity of the films as functions of annealing temperature for both as-deposited and annealed FTO films. It can be observed that all the films are conductive, and as the annealing temperature rises from 500°C to 550°C, the resistivity values decrease for films annealed in a nitrogen atmosphere. This reduction is attributed to the formation of FTO at higher temperatures, which is not achievable at lower temperatures. According to Zoller *et al.* (2019), increased annealing temperatures enhance the crystallinity of the thin films, leading to larger grain sizes and better charge mobility, thus improving electrical performance. However, from 550°C to 600°C, resistivity increases. This suggests at this temperature might introduce defects or alter the microstructure, resulting in poorer conductivity (Guermat, 2019). For samples annealed in open air, resistivity initially increases from 500°C to 550°C but decrease when the temperature reaches 600°C.

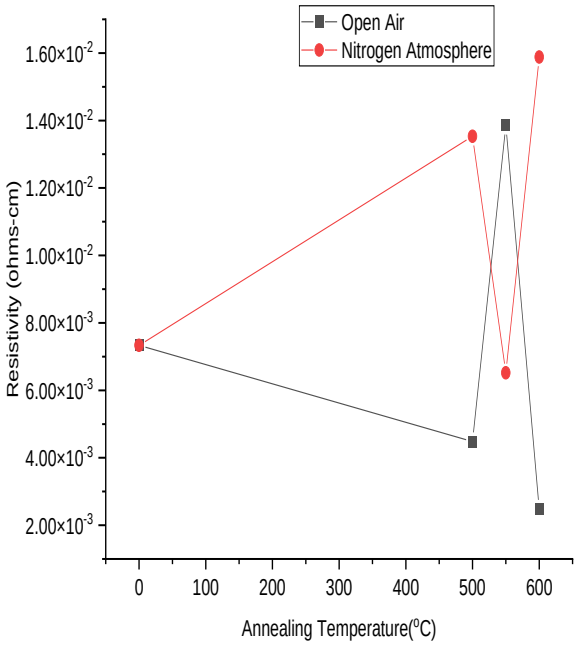

Figure 4: Resistivity versus Annealing Temperature for Films Annealed in Open air and Nitrogen Atmosphere

Figure 5 depicts the variation of sheet resistance (R_{sh}) of FTO thin films with annealing temperature for two different annealing atmospheres (open air and nitrogen).

It can be observed that from the figure, the sheet resistance of as-deposited films at 0°C is approximately $4.99 \times 10^{-2}\Omega$/square which is relatively high due to their amorphous structure. The sheet resistance of thin films annealed at 500°C is lower when annealed in open air compared to those annealed in a nitrogen atmosphere, indicating that air annealing results in better electrical conductivity at this temperature. When the annealing temperature is increased to 550°C, the sheet resistance of the films annealed in air rises significantly. In contrast, the sheet resistance of films annealed in nitrogen decreases at this temperature. This suggests that annealing in nitrogen at 550°C may help stabilize the electrical properties of the films (Zoller *et al.*, 2019). At 600°C, both air and nitrogen annealing lead to reduced sheet resistance, but the decrease is more pronounced for films annealed in nitrogen. This implies that annealing in nitrogen at high temperatures (600°C) may provide the optimal conditions for maximizing the electrical conductivity of the thin films.

DOI: https://doi.org/10.57233/ijsgs.v10i3.699

ISSNp: 2488-9229; **ISSNe:** 3027-1118

IJSGS FUGUSAU VOL. 10 (3) **WEBSITE: https://fugus-ijsgs.com.ng**

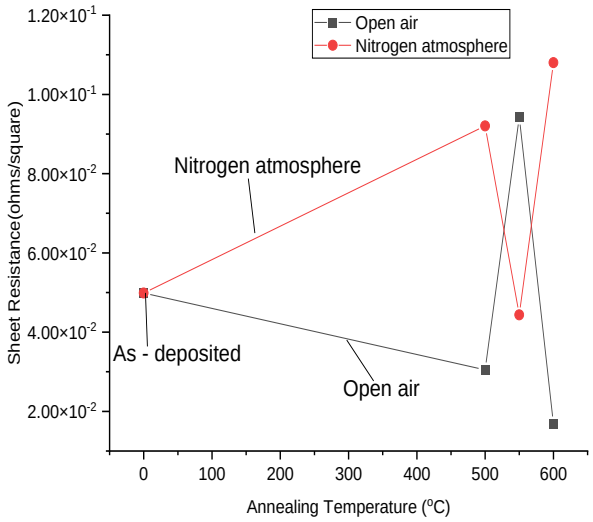

Figure 5: Sheet Resistance against annealing Temperature for Film annealed in Open Air and Nitrogen Atmosphere

Table 2 presents the resistivity (ρ) and sheet resistance (R_{sh}) of FTO (fluorine-doped tin oxide) thin films annealed at various temperatures in different atmospheres (air and nitrogen). Resistivity (ρ) is a measure of how strongly a material opposes the flow of electric current. It is influenced by factors like grain size, defects, and crystallinity of the thin film. Sheet Resistance (R_{sh}) represents the resistance of a thin film that is uniform in thickness. It is defined as the resistivity divided by the thickness of the film and is commonly used for thin films in electronics.

Table 2: Resistivity and Sheet Resistance of FTO Thin Films Annealed at various Annealing Temperatures.

Samples	Resistivity (ρ) (Ω-cm)	Sheet Resistance (R_{sh}) (Ω/square)
As-deposited	7.33×10^{-3}	4.99×10^{-2}
FTO 500°C in air	4.48×10^{-3}	3.05×10^{-2}
FTO 550°C in air	1.39×10^{-2}	9.43×10^{-2}
FTO 600°C in air	2.47×10^{-3}	1.68×10^{-2}
FTO 500°C in N_2	1.35×10^{-2}	9.20×10^{-2}
FTO 550°C in N_2	6.52×10^{-3}	4.44×10^{-2}
FTO 600°C in N_2	1.59×10^{-2}	1.08×10^{-2}

From table 2, the resistivity and sheet resistance for as – deposited FTO thin films are 7.33×10^{-3}Ω-cm and 4.99×10^{-3} Ω/square respectively. The as-deposited FTO film has a relatively high resistivity and sheet resistance, indicating a lower carrier concentration and less efficient conductivity (Yu, *et al*., 2016).

Samples annealed in open air, resistivity for samples annealed at 500°C is 4.48×10^{-3} Ω-cm, at 550°C is 1.39×1010^{-2}Ω-cm and at 600°C is 2.47×10^{-3}Ω-cm. sheet resistance for the same sample in open air are 3.05×10^{-3}Ω/square, 9.43×10^{-2}Ω/square, and 1.68×10^{-2}Ω/square for samples annealed at 500°C, 550°Cand 600°C respectively.

Samples annealed in nitrogen atmosphere, the resistivity for samples annealed at 500°C is 1.35×10^{-3}Ω-cm, at 550°C is 6.52×10^{-2}Ω-cm, and at 600°C 1.59×10^{-2}Ω-cm. sheet resistance for the same sample in nitrogen atmosphere are 9.20×10^{-3} Ω/square, 4.44×10^{-2}Ω/square and 1.08×10^{-2} Ω/square for samples annealed at 500°C, 550°Cand 600°C respectively.

In Air, the annealing at 500°C and 600°C generally improves conductivity (lower resistivity and sheet resistance), suggesting optimal conditions for enhancing the electrical properties of FTO films. However, annealing at 550°C in air shows an increase in resistivity, potentially due to the formation of defects (Yu, *et al*., 2016).

In Nitrogen, The films annealed at 550°C show better conductivity than those annealed at 500°C, implying that nitrogen can affect the microstructure and defect density. However, at 600°C, an increase in resistivity suggests that excessively high annealing temperatures in nitrogen may deteriorate the film's electrical properties (Swathi & Angappane, 2022).

4.0 CONCLUSION

This study examined the effects of annealing temperature on the structural and electrical properties of FTO thin films deposited using the spin coating method and annealed at 500°C, 550°C, and 600°C. The as-deposited sample exhibited an amorphous structure, while the annealed FTO films displayed a SnO_2 phase with crystalline planes (110), (101), (200), (211), and (310), forming a polycrystalline tetragonal structure. Thermal treatment was found to influence the crystallite size of the

DOI: https://doi.org/10.57233/ijsgs.v10i3.699

ISSNp: 2488-9229; **ISSNe:** 3027-1118

IJSGS FUGUSAU VOL. 10 (3) **WEBSITE: https://fugus-ijsgs.com.ng**

FTO thin films, subsequently affecting their electrical properties. The grain size increased with annealing temperature, reaching 15.75 nm, 16.75 nm, and 18.41 nm for films annealed in open air, and 13.04 nm, 12.53 nm, and 15.70 nm for those annealed in a nitrogen atmosphere. This increase in grain size resulted in reduced porosity and lower resistivity values: 4.48×10^{-3} Ω·cm, 1.39×10^{-2} Ω·cm, and 2.37×10^{-3} Ω·cm for samples annealed in open air, and 1.35×10^{-2} Ω·cm, 6.52×10^{-3} Ω·cm, and 1.59×10^{-2} Ω·cm for those annealed in nitrogen. These results suggest that higher annealing temperatures lead to decreased resistivity. The key findings indicate that thermal annealing improves the crystallite size, crystallinity, and electrical conductivity of FTO films, making them an excellent choice for optoelectronic devices and solar cells, among other applications.

REFERENCE

Abdel-Galil, A., Moussa, N. L. and Yahia, I.S., (2021) Synthesis and optical characterization of nanocrystalline fluorine-doped tin oxide films: conductive window layer for optoelectronic applications. Applied Physics A, Springer, https://doi.org/10.1007/s00339-021-04632-4

Adedokun, O., Odebunmi, V. M., & Sanusi, Y. K. (2019). Effect of annealing temperature on structural, optical and electrical properties of spin coated tin oxide thin films for solar cells application. International Journal of Thin Film Science and Technology, 8(3), 157-162.http://dx.doi.org/10.18576/ijtfst/080308

Badawi, A., Althobaiti, M. G., Ali, E. E., Alharthi, S. S., & Alharbi, A. N. (2022). A comparative study of the structural and optical properties of transition metals (M= Fe, Co, Mn, Ni) doped ZnO films deposited by spray-pyrolysis technique for optoelectronic applications. Optical Materials, 124, 112055. https://doi.org/10.1016/j.optmat.2022.112055

Dharmaprakash, S. M. (2023). Transparent and conductive thin films of cadmium doped tin oxide fabricated by pulsed laser deposition technique. Physica B: Condensed Matter, 665, 415059. https://doi.org/10.1016/j.physb.2023.415059

Elanjeitsenni, V. P., Vadivu, K. S., & Prasanth, B. M. (2022). A review on thin films, conducting polymers as sensor devices. Materials Research Express, 9(2), 022001. **DOI** 10.1088/2053-1591/ac4aa1

El Jouad, M., Gaumer, N., Touhtouh, S., & Hajjaji, A. (2023). Structural, optical behavior and Judd-Ofelt analysis of europium-doped silicophosphate glasses for red-emitting device applications. Journal of Luminescence. 256, 119640. https://doi.org/10.1016/j.jlumin.2022.119640

Ethiraj, A. S., Rhen, D. S., Soldatov, A. V., Ali, G. A., & Bakr, Z. H. (2021). Efficient and recyclable Cu incorporated TiO2 nanoparticle catalyst for organic dye photodegradation. Int. J. Thin Film Sci. Technol, 10, 169-182. http://dx.doi.org/10.18576/ijtfst/100306

Gholami, M., Tajabadi, F., Taghavinia, N., & Moshfegh, A. (2023). Chemically-stable flexible transparent electrode: gold-electrodeposited on embedded silver nanowires. Scientific Reports.13(1), 17511. https://doi.org/10.1038/s41598-023-44674-7

Guermat, N. (2019, November). Deposition times influence on properties of 8 wt% Fluorine–doped Tin Oxide thin films deposited by spray pyrolysis. In International conference on Mechanics and Materials (ICMM19) Sétif. (Vol. 11, p. 12). DOI: 10.1007/s10854-020-04936-w

Harilal, S. S., Phillips, M. C., Froula, D. H., Anoop, K. K., Issac, R. C., & Beg, F. N. (2022). Optical diagnostics of laser-produced plasmas. Reviews of Modern Physics, 94(3), 035002. https://doi.org/10.1103/RevModPhys.94.035002

Ikpesu, J. E., Iyuke, S. E., Daramola, M., & Okewale, A. O. (2020). Synthesis of improved dye-sensitized solar cell for renewable energy power generation. Solar Energy, 206, 918-934.https://doi.org/10.1016/j.solener.2020.05.002

Kadhim, K. R., & Mohammed, R. Y. (2022). Effect of annealing time on structure, morphology, and optical properties of nanostructured CdO thin films prepared by CBD technique. Crystals, 12(9), 1315. https://doi.org/10.3390/cryst12091315

Kajal, R., Kataria, B. R., Asokan, K., & Mohan, D. (2023). Effects of gamma radiation on structural, optical, and electrical properties of SnO2 thin films. Applied Surface Science Advances, 15, 100406. https://doi.org/10.1016/j.apsadv.2023.100406

Khemiri, N., Chamekh, S., & Kanzari, M. (2020). Properties of thermally evaporated CZTS thin films and numerical simulation of earth abundant and non toxic CZTS/Zn (S, O) based solar cells. Solar Energy, 207, 496-502. https://doi.org/10.1016/j.solener.2020.06.114

Kim, J., Wong, S., Kim, G., Park, Y. B., van Embden, J., & Della Gaspera, E. (2020). Transparent electrodes based on spray coated fluorine-doped tin oxide with enhanced optical, electrical and mechanical properties. Journal of Materials Chemistry C, 8(41), 14531-14539. https://doi.org/10.1039/D0TC03314F

Muhammad, Z. A., & Alwan, T. J. (2020). Optical properties and FT-IR spectra of PANI/f-MWCNT thin films. Experimental and Theoretical Nanotechnology, 23(1), 47-55. DOI: 10.56053/5.1.47

DOI: https://doi.org/10.57233/ijsgs.v10i3.699

ISSNp: 2488-9229; **ISSNe:** 3027-1118

IJSGS FUGUSAU VOL. 10 (3) **WEBSITE: https://fugus-ijsgs.com.ng**

Park, J., Park, T., Kim, Y. J., & Yoo, H. (2024). Light-induced, room-temperature hydrogen gas detection based on SnO2 quantum Dots/p-Si. Applied Surface Science, 670, 160693. https://doi.org/10.1016/j.apsusc.2024.160693

Sabzehmeidani, M. M., Gafari, S., & Kazemzad, M. (2024). Concepts, fabrication and applications of MOF thin films in optoelectronics: A review. Applied Materials Today, 38, 102153. https://doi.org/10.1016/j.apmt.2024.102153

Shekhirev, M., Shuck, C. E., Sarycheva, A., & Gogotsi, Y. (2021). Characterization of MXenes at every step, from their precursors to single flakes and assembled films. Progress in Materials Science, 120, 100757. https://doi.org/10.1016/j.pmatsci.2020.100757

Swathi, S. P., & Angappane, S. (2022). Enhanced resistive switching performance of hafnium oxide-based devices: Effects of growth and annealing temperatures. Journal of Alloys and Compounds, 913, 165251. https://doi.org/10.1016/j.jallcom.2022.165251

Tofighi, G., Degler, D., Junker, B., Müller, S., Lichtenberg, H., Wang, W. & Grunwaldt, J. D. (2019). Microfluidically synthesized Au, Pd and AuPd nanoparticles supported on SnO2 for gas sensing applications. Sensors and Actuators B: Chemical, 292, 48-56. https://doi.org/10.1016/j.snb.2019.02.107

Yu, S., Li, L., Lyu, X., & Zhang, W. (2016). Preparation and investigation of nano-thick FTO/Ag/FTO multilayer transparent electrodes with high figure of merit. Scientific reports, 6(1), 20399. https://doi.org/10.1038/srep20399

Yu, S., Zhao, L., Liu, R., Wu, M., Sun, Y., & Li, L. (2019). Electrical properties of bulk and interface layers in Sb doped SnO2 thin films. Ceramics International, 45(2), 2201-2206. https://doi.org/10.1016/j.ceramint.2018.10.131

Zoller, F., Böhm, D., Bein, T., & Fattakhova-Rohlfing, D. (2019). Tin oxide based nanomaterials and their application as anodes in lithium-ion batteries and beyond. ChemSusChem, 12(18), 4140-4159. https://doi.org/10.1002/cssc.201901487